

Phenothiazine Dimer as Efficient and Recyclable p-Type Organic Positive Electrode Material for Anion-Ion and Dual-Ion Batteries

Murugesan Rajesh, Seynabou Diallo, Yann Danten, Carlo Gatti, Christine Frayret, Sylvestre Toumieux, and Matthieu Becuwe*

This article presents the electrochemical properties of a series of phenothiazine and phenoxyazine dimers, by involving an aromatic central core, efficiently synthesized in a single step through a Buckwald–Hartwig coupling reaction. A synergistic approach combining experimental and quantum chemical studies was used in view of providing a thorough characterization of their capabilities as electrodes in the context of electrochemical energy storage applications. A detailed study of the electrochemical activity was then conducted with the aim of optimizing performance, i.e.,

achieving a specific capacity of around 100 mAh.g^{-1} , close to the theoretical values at a potential of 3.6 V relative to Li metal. The dimerization strategy also emerged as an interesting methodology, since it gives rise to molecular materials having specific solubility properties. This finding opens up the possibility of recovering the active material from the electrode at the end of its life, thus paving the way for improved organic electrodes and batteries, especially with respect to their recyclable character.

1. Introduction

The exceptional demand for energy storage devices of various types, shapes, and applications is creating a global dynamic that highlights geopolitical issues related to the origin and availability of critical raw materials and elements, as well as the locations of their manufacturing.^[1] A key concern for researchers is now to

identify new alternatives for developing energy storage devices that both overcome these limitations while being obtained through a more sustainable way. Substituting traditional critical elements, primarily used as intercalation compounds, with redox-active organic materials (ROMs) has been considered one of the most promising ‘greener’ alternatives in rechargeable batteries, due to the greater abundance of organic compounds based on earth-abundant elements (C, H, N, O, and S).^[2] Moreover, ROMs also provide high structural/chemical diversity, tunable redox electrochemistry and simplified end-of-disposal compared to their inorganic counterparts, making them high prospects to be applied as energetic electro-active materials in various types of batteries (Li, Na, or K ion).^[3–5] Additionally, ROMs offer the probability to frame the battery setup with various types of ions, thereby advancing the freedom in the selection of charge carriers in the electrolyte and opening the way toward battery without any metal elements.

Electrode materials involving *p*-type molecules are at the forefront of attention, as they pave the way for materials free of critical elements (including lithium), since anions can be used as charge carriers between the electrodes. This fact is important because the anion can be chosen from a wide range of compounds made from abundant elements, for which the issue of criticality is nearly irrelevant. Another pertinent point is the absence of dendrite formation in this type of battery. Extensive research in recent years has led to the identification of various promising ROMs, such as phenazine, phenoxyazine, thianthrene, and carbazole derivatives, that can be used as *p*-type positive electrode materials for energy storage.^[6–13]

Phenothiazine contributes to a remarkable improvement in performance in terms of a higher voltage profile with multi-electron activity, notable long-term stability, and a scalable

M. Rajesh, S. Diallo, C. Frayret, M. Becuwe
Laboratoire de Réactivité et de Chimie des Solides
UMR CNRS 7314

Université de Picardie Jules Verne
Amiens Cedex 1 F-80039, France
E-mail: matthieu.becuwe@u-picardie.fr

M. Rajesh, S. Diallo, C. Frayret, M. Becuwe
Réseau sur le Stockage Electrochimique de l’Energie (RS2E)
FR CNRS 3459

Amiens 80039, France

S. Diallo, S. Toumieux
Laboratoire de Glycochimie et des Agro-ressources d’Amiens (LG2A)
UR 7378 Université de Picardie Jules Verne (UPJV)
10 rue Baudelocque, Amiens 80039, France

Y. Danten
Institut des Sciences Moléculaires
UMR CNRS 5255
Talence 33405, France

C. Gatti
CNR SCITEC
CNR Istituto di Scienze e Tecnologie Chimiche “Giulio Natta”
20100 Milano, Italy

 Supporting information for this article is available on the WWW under <https://doi.org/10.1002/batt.202500403>

 © 2025 The Author(s). *Batteries & Supercaps* published by Wiley-VCH GmbH. This is an open access article under the terms of the Creative Commons Attribution License, which permits use, distribution and reproduction in any medium, provided the original work is properly cited.

platform for the development of electron-donating *p*-type materials. In general, small-molecule phenothiazine derivatives are rarely used as electrode materials in batteries due to their significant dissolution problem in liquid electrolytes. To address this problem, focus was made on the design of novel phenothiazine-based redox-active polymers as positive electrode materials.^[14–18] The molecular approach is still an interesting option to boost specific capacity and, consequently, push phenothiazine compounds to the forefront of materials to be used in energy storage devices in the future. In this context, one of the main challenges for phenothiazine is to develop efficient molecular-based compounds, for which the synthesis pathway requires a limited number of steps, while also demonstrating good electrochemical performance, excellent stability, and tunable solubility to maximize storage capacity.

To achieve this goal, introducing functional groups or expanding the aromatic π -conjugation via molecular engineering can correspond to valuable strategies thanks to a significant modulation of various aspects, including the solubility, the electronic conductivity, and the electrochemical performance of small organic molecules. This molecular engineering approach was successfully applied to improve performance of molecular phenothiazine in organic-based electrolyte for anion-ion or dual-ion batteries.^[8,19]

Here, we present the electrochemical properties of a series of *p*-type organic molecular positive electrode materials based on *N*-substituted phenothiazine (PT) or phenoxazine (PZ) dimers, linked by an aromatic core, and synthesized through a one-step process (Figure 1a). The dibromobenzene derivatives (1,4-dibromobenzene or 1,4-dibromo-2,5-dimethylbenzene) was easily coupled with phenothiazine (PT) or phenoxazine (PZ) electroactive groups through a palladium Buchwald–Hartwig C–N cross-coupling using bis(*tri-tert*-butylphosphine) palladium (0) as catalyst (5 mol%) and potassium phosphate as a base under reflux until complete conversion (see ESI for synthesis details and Scheme S1, Supporting Information). The four dimers (PT, MPT, PZ, and MPZ), whose labeling is described hereafter, were obtained in good yield ranging from 79 to 87% and good purity (see Figure S1–8, Supporting Information). Phenothiazine/phenoxazine dimers holding a hydrogen (PT/PZ) or *para*-dimethyl (indicated here for the sake of simplicity as “M”) group (MPT/MPZ)

on the aromatic core show specifically promising redox potential, i.e., $E^\circ = 3.6$ V/Li⁺ (Figure 1b) for positive electrode applications. Noteworthy, performances and capacities depend upon the content of conductive additives and electrolyte salt, as these factors presumably influence the physicochemical properties of the material and, therefore, its retention capacity, due to delamination and/or solubility phenomena. As a key highlight, molecular electrode materials have been successfully recycled after various electrochemical tests, thanks to their specific solubility in dichloromethane. Indeed, without any other specific treatments except the removing of this solvent used during the extraction, organic electrode materials were reprocessed in new battery cells, demonstrating their high stability as well as their high potential for materials sustainability owing to an easy, low-energy recycling, therefore reducing the need to synthesize new derivatives.

2. Results and Discussions

Firstly, electrochemical tests using Galvanostatic Cycling with Potential Limits (GCPL) were carried out on the four dimers synthesized (Figure 2a–d up). The electrochemical signal was very similar in each case and showed an average redox potential of 3.6 V vs. Li⁺/Li⁰ for all the dimers. In most cases, the theoretical specific capacity (Figure 2a–d bottom) is reached during first oxidation with 97 mAh.g^{−1}, 132 mAh.g^{−1}, 116 mAh.g^{−1}, and 128 mAh.g^{−1} for PT, MPT, PZ, and MPZ dimer respectively. On the other hand, the extra capacity at the beginning for the derivatives could be explained by both conductive carbon contribution and by the attack of a second electron leading to the irreversible oxidation of chalcogen atom (S or O), explaining as well the poor coulombic efficiency (Figure S9–10, Supporting Information). Despite this aspect, dimers holding two methyl groups in positions 2 and 5 of the aromatic core show better capacity retention over 100 cycles, with 104 and 99 mAh.g^{−1} for MPT and MPZ dimers respectively (Figure 2b and c bottom), while PT and PZ show specific capacities of 52 and 63 mAh.g^{−1} respectively. This observation suggests that the methyl group could play a certain role in the electrochemical reaction.

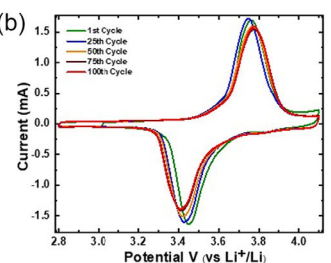
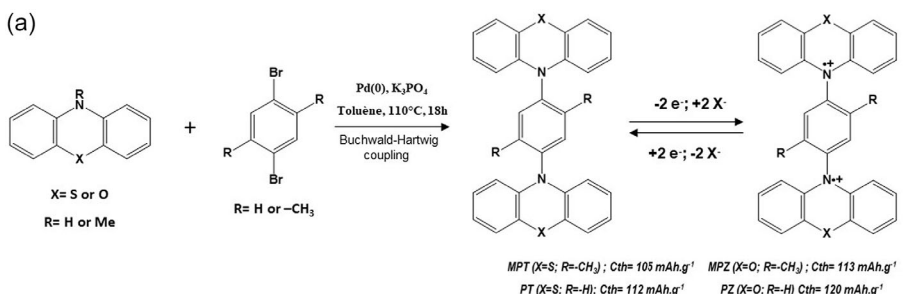


Figure 1. a) General synthesis pathway for redox-dimer and expected two-electron redox mechanism associated with theoretical gravimetric capacities. b) Example of electrochemical activity of redox-dimer (case of 70% composite of MPT dimer) obtained by cyclic voltammetry performed over 100 cycles at cyclic rate of 0.1mV/s between 2.8 and 4.1 V vs. Li metal using 1 M LiClO₄ in propylene carbonate as electrolyte.

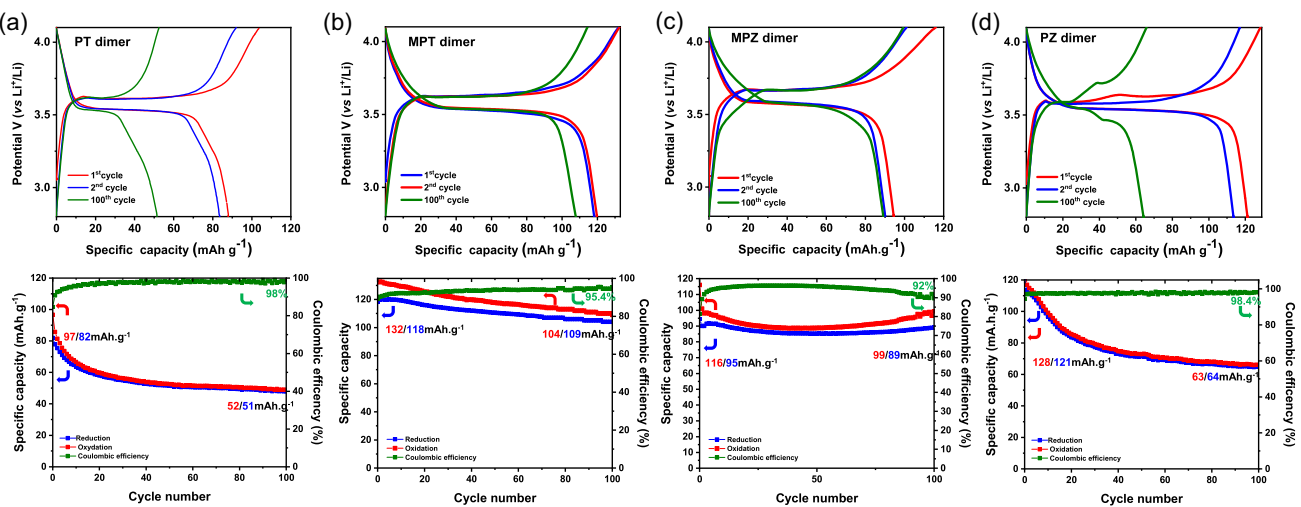


Figure 2. Electrochemical profile for the first, second and hundredth cycle (up), corresponding specific capacities and coulombic efficiency (bottom) for redox-dimer based on phenothiazine a) and b) and phenoxazine c) and d) composites (70% of active material) galvanostatically cycled over 100 cycles at C/10 rate between 2.8 and 4.1 V vs. Li metal and using 1 M LiClO₄ in propylene carbonate as electrolyte (up).

Based on this, attention was focused on phenothiazine dimers only in the following.

As a preliminary step toward understanding the electrochemical properties of some of the abovementioned compounds (Figure 1) and following a first set of calculation on simple phenothiazine core (Figure S11, Table S1, Scheme S2, Supporting Information), a molecular DFT investigation was undertaken on simple phenothiazine core to set-up with the aim of examining the evolution of the structural and electronic properties of these representative species upon single (or mono-) and double or d-oxidation processes. The considered 1,4-phenylene-bis phenothiazine derivatives (i.e., PT and MPT dimers) contain two phenothiazine (PTZ) moieties (PTZ-1 and PTZ-2) well-separated by a 6-membered ring (6MR). The singlet, doublet, and triplet (ground) states, representing the spin multiplicities of the various envisaged oxidized forms, are labeled S₀, D₀, and T₀, for nonoxidized, singly oxidized and doubly oxidized compounds, respectively.

Focusing on the various derivatives computationally examined, distinct structural aspects can first be noticed according to the study of the calculated structures of the phenothiazine (PT and MPT) dimers, represented in various oxidation states on Figure 3. They are detailed in the ESI section (Table S2–3, Figure S12, Scheme S3–4, Supporting Information). As a noticeable effect, singly oxidized (SO) species, i.e., radical cationic (D₀⁺) structures obtained through the removal of one electron from the dimer system (either PT or MPT), tend to present a structural effect of planarity that is strictly confined to only one of the two PTZ sections. Conversely, the two PTZ sections of the T₀^{•+2} biradical dicationic form of the PT or MPT compounds both exhibit a quasi-planar geometry.

Additionally, when considering the oxidized states of the PT dimer, it can be observed that Φ(6MR, PTZ-1) and Φ(6MR, PTZ-2) are no longer equal to zero in these forms. Specifically, for the doubly oxidized T₀^{•+2} state of this compound, these values are 5.5° and 5.0°, respectively, while for the corresponding singly

oxidized D₀⁺ state, the changes compared to the nonoxidized S₀ state are less pronounced, these values being 1.0° and 3.0°, respectively. In contrast, for the MPT dimer, the situation is different. PTZ-2 is unaffected by oxidation in relation to the Φ angle, which remains zero for both the D₀⁺ and T₀^{•+2} states. For PTZ-1, it is extremely close to zero, with a value of −0.1° for both the singly and doubly oxidized states. These various results, dealing with characteristics of Φ(6MR, PTZ-1 or 2), might explain why the MPT dimer seems to exhibit better reversibility in the electrochemical reaction and improved capacity retention, as will be described hereafter.

By further progressing in the analysis, focusing now on the electronic structure aspects, it is worth noting that the trends mentioned earlier, based on the evolution of geometric features, are confirmed. This is clearly demonstrated by the spin density distribution maps (Figure 4). In the case of the singly oxidized radical cationic (D₀⁺) species of PT or MPT dimer, it is evident that the spin density is confined to one of the two PTZ units. In contrast, for the corresponding doubly oxidized biradical dicationic states (T₀^{•+2}) of these compounds, the spin density is distributed across both PTZ units. Specifically, for the singly oxidized state of PT dimer (D₀⁺), the spin density is predominantly localized on the PTZ-1 fragment, with particular concentration on C_{ring 1} (i.e., all C atoms from ring 1), C_{ring 2} (i.e., all C atoms from ring 2), and the S and N atoms, with atomic population values of ≈0.233, 0.232, 0.277, and 0.250 e[−], respectively. The situation is very similar for the MPT dimer in the same state, with atomic population values of ≈0.232, 0.232, and 0.276 and 0.251 e[−] for the same types of atoms. In the case of the doubly oxidized PT dimer state (T₀^{•+2}), the spin density distribution clearly indicates the location of oxidation, which now spans both PTZ units. The atomic population values are ≈0.233, 0.233, 0.281, and 0.246 e[−] in PTZ-1 and ≈0.233, 0.233, 0.281, and 0.246 e[−] in PTZ-2 for C_{ring 1}, C_{ring 2}, S, and N atoms, respectively.

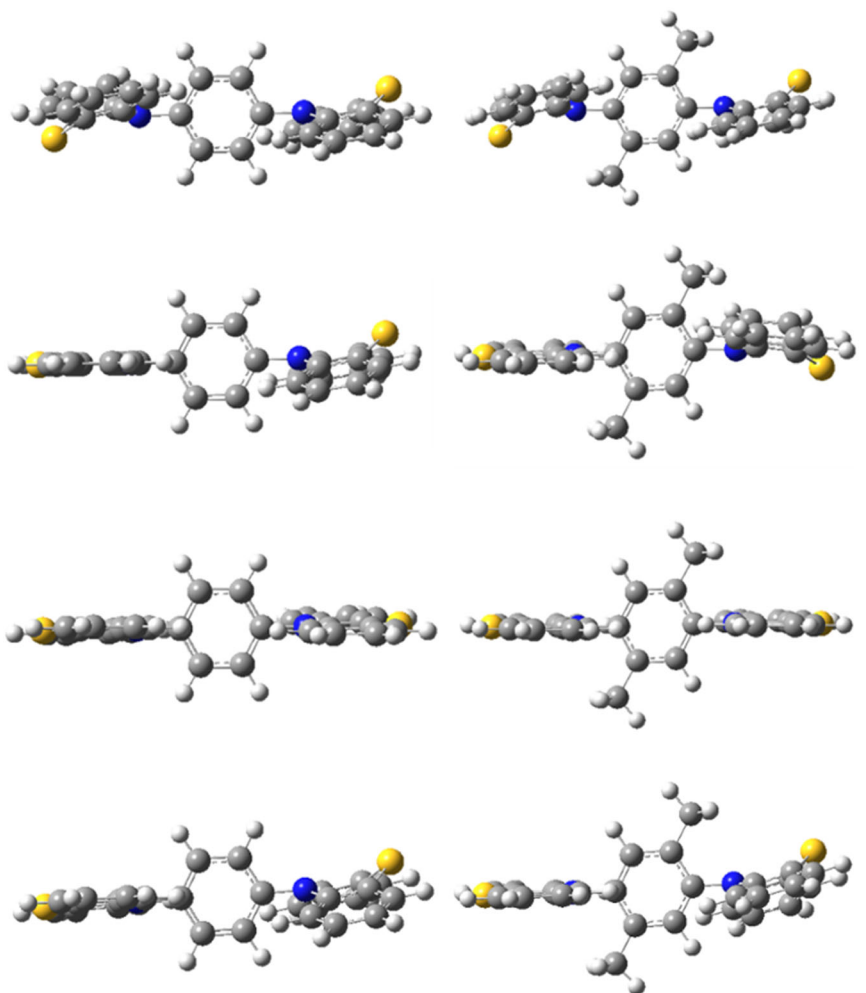


Figure 3. From top to bottom, representative structures of the phenothiazine dimers (PT (on left) and MPT (on right) in various oxidation states: i) first line: in neutral nonoxidized (S_0) state; ii) second line: radical cationic singly oxidized ($D_0^{\cdot+}$) state; iii) third line: biradical dicationic doubly oxidized ($T_0^{\cdot\cdot+2}$) state; iv) dicationic doubly oxidized (S_0^{2+}) state, the latter being displayed just for a thorough indication since these forms were found to be significantly less stable than their biradical dicationic ($T_0^{\cdot\cdot+2}$) counterparts.

The same observations apply to the $T_0^{\cdot\cdot+2}$ state of the MPT dimer, for which values very similar to those in the PT case are observed: ≈ 0.232 , 0.232 , 0.280 , and 0.247 e^- in PTZ-1, and ≈ 0.232 , 0.232 , 0.280 , and 0.247 e^- in PTZ-2 for $C_{\text{ring } 1}$, $C_{\text{ring } 2}$, S, and N atoms, respectively. Despite the fact that these two successive one-electron redox processes are usually considered for phenothiazines as an oxidation occurring first on nitrogen (N) atom and then on sulfur (S) atom, it is striking to observe in the two examined dimer species that the above-mentioned spin density distribution seems to preclude a predominant form of a radical cation positioned precisely on nitrogen at the singly oxidized state. The lack of marked differentiation between $D_0^{\cdot+}$ and $T_0^{\cdot\cdot+2}$ states concerning spin density distribution on N and S also reinforces this conclusion. In fact, one can notice a slightly larger/lower spin density distribution on sulfur/nitrogen by switching from $D_0^{\cdot+}$ to $T_0^{\cdot\cdot+2}$ states, but the difference is tiny (≈ 0.003 – 0.004 e^-). Therefore, the collected results for single and double oxidation of PT and MPT tend to advocate for nearly identical contributions from the nitrogen (N) and sulfur (S) redox

centers in both oxidation states, owing to efficient π -electron delocalization.

Further investigations were conducted on MPT dimer. First, various carbon additive contents in the composite were tested (Figure 5). Attempts were made to reduce the conductive additive content to 20% in the powder composite (with 80% active material), and the results showed that the material still exhibited promising capacity at the beginning, with 109 mAh g^{-1} for the first oxidation (Figure 5a). Nonetheless, the capacity recovered during the first reduction is lower than that for the 70% composite. The second cycle shows a 10% capacity fading compared to the first, and the signal appears more polarized. Over 25 cycles, while the capacity in oxidation is stable (90 mAh g^{-1}), a 20% capacity fading is observed for the reduction, accompanied by significant polarization (600 mV) in the electrochemical curves, suggesting conductivity issues. A similar trend is observed at higher cycling rate (C/4) during the first 25 cycles (Figure 5b). Interestingly, a slight increase in capacity is observed up to 50 cycles, followed by a continuous capacity

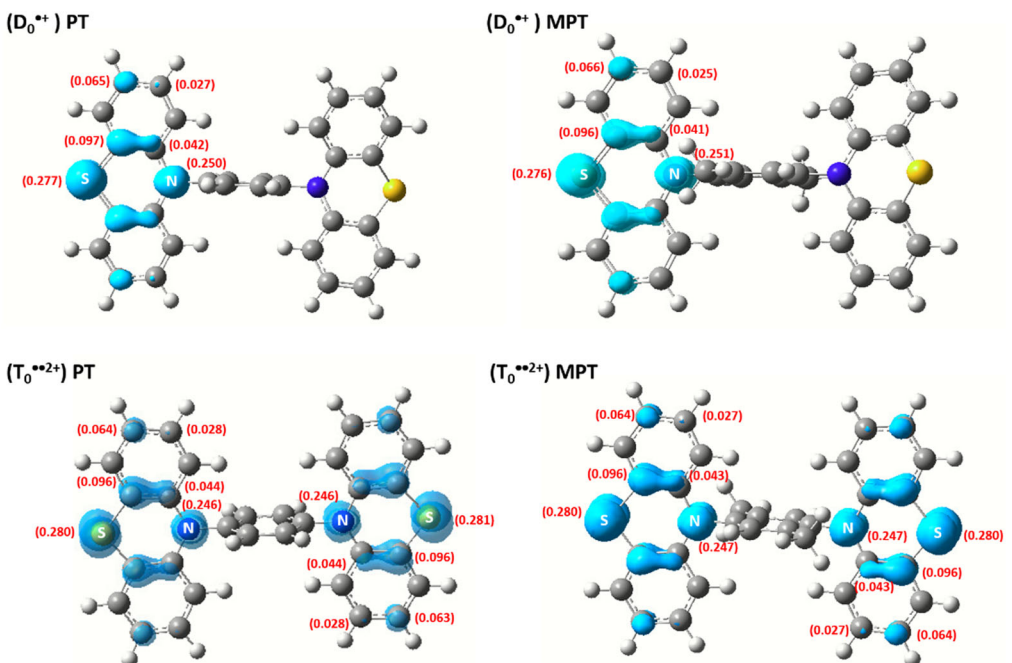


Figure 4. Spin density distributions maps for i) on top: singly oxidized ($D_0^{\bullet+}$) PT (left) and MPT (right); ii) at the bottom: doubly oxidized ($T_0^{\bullet\bullet 2+}$) PT (left) and MPT (right).

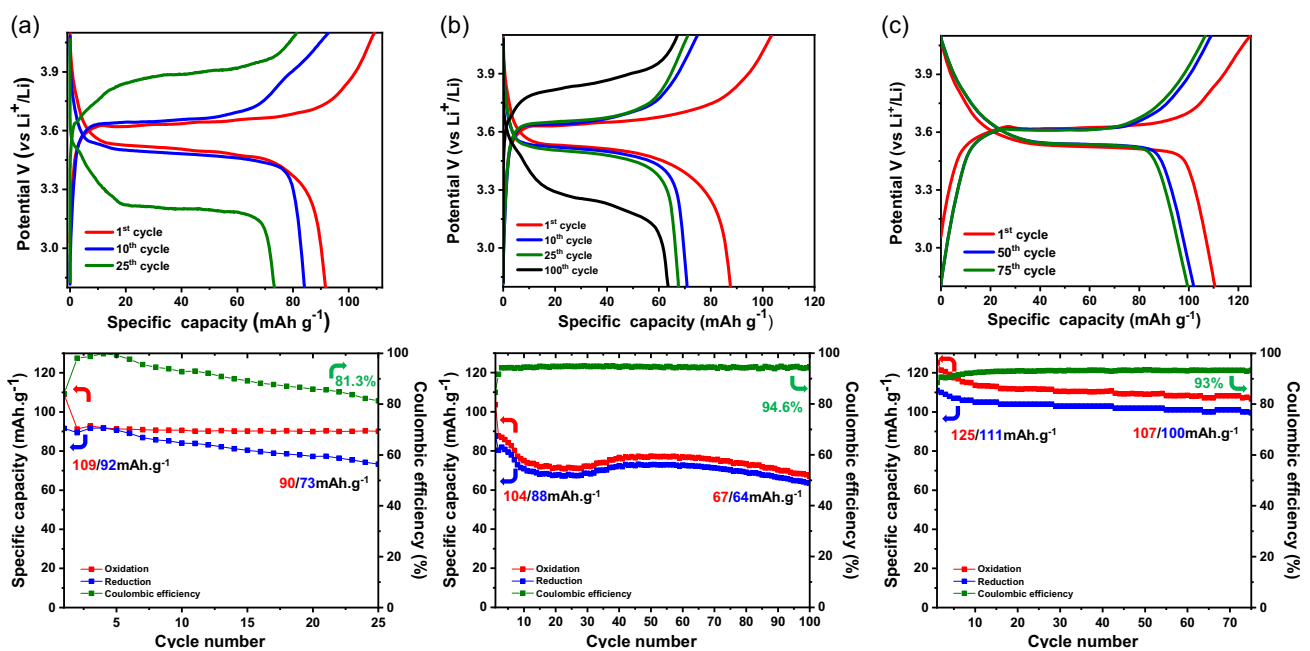


Figure 5. Electrochemical activity (up), capacity retention (bottom), and Coulombic efficiency (bottom) of MPT dimer composite composed of 80% a) and b) or 60% c) of active material, galvanostatically cycled at C/10 (a) and (c) or C/4 (b) rate between 2.8 and 4.1 V vs. Li metal and using 1 M LiClO₄ in propylene carbonate as electrolyte.

fading (64/67 mAh g⁻¹ after 100 cycles), with higher polarization (around 600 mV) but the Coulombic efficiency remains quite stable (at nearly 95%). On the other hand, when the additive content is increased to 40% (60% of active mass), no capacity fading is observed, and the electrochemical performance is quite similar to the previous results obtained for the 30%

composite, though with still low Coulombic efficiency due to the irreversible redox reaction of the chalcogen atom (Figure 5c). This suggests that the capacity fading observed earlier is more related to conductivity issues than to material solubilization. Thus, the 30% additive composite was found to be the best compromise.

Another interesting parameter to investigate is the electrolyte salt, particularly the anion. Since the electrochemical reaction involves the insertion/disinsertion of anions, it is crucial and interesting to determine which anion is the most effective. Although no clear trend emerges for selecting a specific anion with the material, few studies highlight the significance of anion size and properties in the electrochemical response^[20]. Based on previous studies, perchlorate (ClO_4^-) represents generally the best choice for maximizing performance,^[19] which also justifies its use in this study. To complete this, two other anions, PF_6^- and TFSI^- , were tested. As shown in the galvanostatic cycling results, the signal is more or less influenced by the choice of anion (Figure 6). Transition from ClO_4^- to PF_6^- leads to a specific capacity decay to a lower value (117/93 mAh g⁻¹ vs. 132/118 mAh g⁻¹) and a 20% decrease in Coulombic efficiency (from 95% to 75%). Polarization is also slightly affected, increasing from 90 to 110 mV (Figure 6a,b).

The use of the TFSI^- anion induces a significant change in the electrochemical response (Figure 6c). Firstly, a specific capacity of 151 mAh g⁻¹ can be noted during the first oxidation. At this stage, it is difficult to pinpoint the exact origin of this activity, but since the TFSI anion is stable at this redox potential, it is plausible to ascribe it to the ROM material. One possibility is that the second redox equilibrium (involving S atom), which typically occurs at a potential of 4.1 V vs. Li metal, is 'lowered' by the insertion of the first TFSI anion during the oxidation of the nitrogen atom (disturbance of the electron density of the redox center). This hypothesis is further supported by the fact that this activity rapidly diminishes after the second cycle (irreversible electrochemical process) and additional electrochemical test with narrower and

broader potential window (see Figure S9, Supporting Information). Over the first two cycles, the Coulombic efficiency is low (less than 50%), but it improves in subsequent cycles. The specific capacity then stabilizes at around 50 mAh g⁻¹.

Since the perchlorate anion yielded the best results, further tests were carried out at higher cycling rates to evaluate the compound's performance (Figure 7 and S13–14, Supporting Information). As expected, increasing the cycling rate resulted in a decrease in the specific gravimetric capacity (in oxidation), which dropped from 109 to 43 mAh g⁻¹ as the cycling rate increased from C/10 to 2C (Figure 7a). The higher cycling rate also led to a significant increase in Coulombic efficiency, which reached 97% at 2C (up from 83% at C/10), suggesting potential dissolution of the active material during the electrochemical reaction. When the rate was reduced back to C/10, the specific capacity increased to 90 mAh g⁻¹ but then decreased to 82 mAh g⁻¹ after 55 cycles (Figure 7b). The Coulombic efficiency also decreased but stabilized at 91%. At a C/4-rate, after reaching a pseudo-steady state until the 150th cycle (58 mAh g⁻¹), the trend remained consistent over 800 cycles, showing a gradual decrease to 31 mAh g⁻¹ (Figure 7c).

These results suggest that the loss of electrode capacity, which depends on the applied regime, could be attributed to the solubilization or delamination of the active material in the electrolyte.^[21] At this stage, it is difficult to make further progress, as changing the solvent does not significantly improve performance, and a solvent-free solid electrolyte solution capable of conducting ClO_4^- -type anions is not yet available.

Although the partial dissolution of the active material requires further investigation and a change in electrolyte to stabilize the

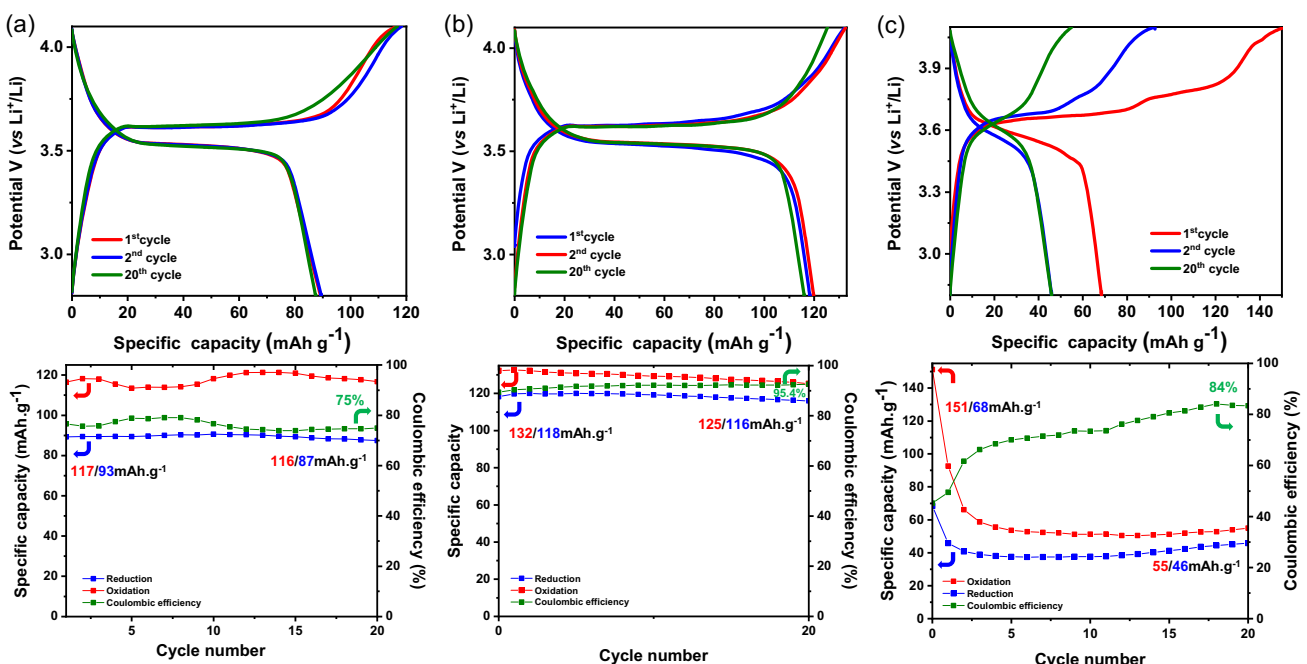


Figure 6. Electrochemical activity (up), capacity retention (bottom) and Coulombic efficiency (bottom) of MPT dimer composite (70% of active material) galvanostatically cycled at C/10 a) and c) or C/4 b) rate between 2.8 and 4.1 V vs. Li metal and using 1 M LiPF₆ (a), 1 M LiClO₄ (b) or 1 M LiTFSI (c) in Propylene Carbonate as electrolyte.

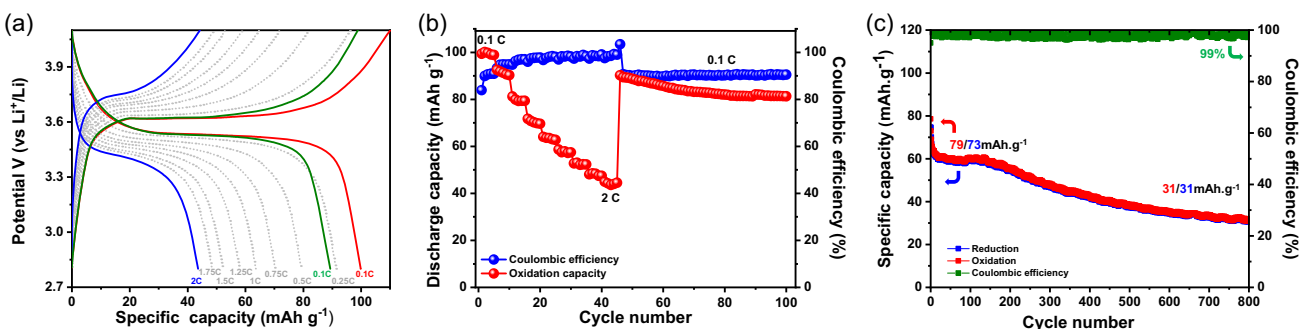


Figure 7. Galvanostatic profile a) and discharge specific capacity over 100 cycles b) of MPT dimer composite (70% of active material) galvanostatically cycled from 0.1 to 2 C rate between 2.8 and 4.1 V vs. Li metal and using 1 M LiClO₄ in propylene carbonate as electrolyte. Capacity retention (red and blue) and Coulombic efficiency (green) of MPT dimer composite composed of 70% active material, galvanostatically cycled at C-rate over 800 cycles c) between 2.8 and 4.1 V vs. Li metal and using 1 M LiClO₄ in propylene carbonate as electrolyte.

material's promising performance, this property presents an excellent opportunity for recycling. To this end, initial recycling trials have been carried out on composites of various origins (**Figure 8**). A composite electrode (70% active material) was first galvanostatically cycled 5 times under the same conditions as those used in the previous tests (Figure 8a). The electrode was then recovered and dissolved in an organic solvent (dichloromethane in this case). The organic phase was filtered to remove solid particles (conductive additive) and subsequently evaporated. The amount recovered was relatively small (\approx 10 mg) nevertheless with good purity based on NMR analysis and was sufficient to recast the composite and assemble a new cell. The "Recycled" composite electrode exhibits the electrochemical signal of the active material at 3.6 V vs. Li, with a reversible capacity of 60 mAh g^{-1} within the potential range of 2.8–3.9 V vs. Li, which is a very encouraging result. The procedure was then repeated using a composite electrode that had been initially cycled 23 times. The results were similar, except that the capacity obtained for the first redox equilibrium was higher ($70\text{--}80 \text{ mAh g}^{-1}$). This difference between the two tests can be attributed to the possible presence of salt in the recovered compound, residual electrolyte solvent, and inactive degradation products (Figure S15–16, Supporting Information). Surprisingly, a second

redox phenomenon was observed at 4.08 V vs. Li, which was not present initially. This phenomenon is similar to the irreversible oxidation of the sulfur atom in the dimer. It is likely due to differences in particle size, and therefore to the resistivity of the active material, which causes a change in the polarization of the signal.

A second recycling test was also carried out, but this time using several electrochemical cells from different tests (GCPL, power curve, long-term and high-rate cycling). Similar to the recycled composite from the initial material cycled 23 times, the 'recycled' composite, now galvanostatically cycled at a C/4 rate, exhibited reversible redox activity at 3.6 V vs. Li and irreversible activity between 3.9 and 4.1 V vs. Li (Figure 8b). This again suggests an irreversible redox reaction of the sulfur atom in the phenothiazine unit. Another point of interest is the evolution of the specific capacity of the recycled composite, which remains relatively stable, although it decreases from 80 mAh.g^{-1} (1st oxidation at 150 mAh.g^{-1}) to 65 mAh.g^{-1} after 300 cycles (Figure 8c). Also noteworthy is the stable Coulombic efficiency of 97% over 300 cycles, starting from cycle 25 onwards.

These differences in reactivity can certainly be ascribed to variations in crystallinity or particle size or can originate from the presence of impurities in the recycled material. For example, the presence of salt may not be detectable by NMR, which could

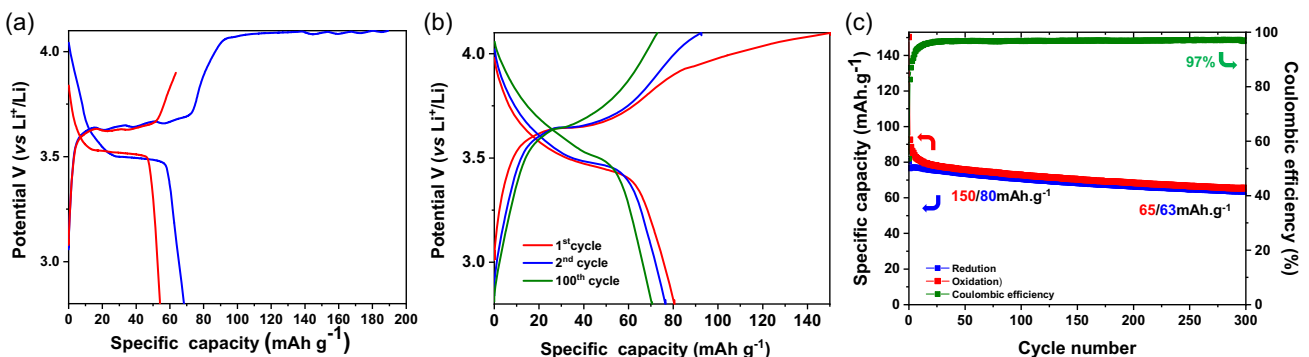


Figure 8. Galvanostatic profiles obtained for composites (70% active material) based on recycled MPT initially tested during 5 cycles (red curve) and 23 cycles (blue) metal using 1 M LiClO₄ in propylene carbonate as electrolyte a) Electrochemical activity b) capacity retention and Coulombic efficiency c) of MPT dimer composite (70% of active material), obtained from the recycling of active material of four differently cycled cells (GCPL, power curve, high-rate cycling...) galvanostatically cycled at C/4 rate between 2.8 and 4.1 V vs. Li metal using 1 M LiClO₄ in propylene carbonate as electrolyte.

result in inaccuracies in the mass of active material present in the composite. However, this preliminary study demonstrates that it is possible to recover active material relatively efficiently. It highlights the need for more in-depth studies, including those focused-on chemistry and process engineering.

3. Conclusion

With the goal of designing next-generation molecular organic electrode materials, an exploration of electrochemical properties of a series of phenothiazine and phenoxazine dimers was carried out. Using DFT calculations, selection among phenothiazine dimers was narrowed, this class of compounds being found otherwise to offer superior retention capacity compared to phenoxazine dimers. Some relevant indices concerning the mechanisms involved in either single or double oxidation processes were gained thanks to both structural aspects and spin density distributions. After studying various external parameters, including the content of conductive additive and the type of electrolyte, specific capacities that reached the theoretical value were obtained. Combined with a redox potential of 3.6 V compared with Li metal, these results position this type of materials as a prime candidate for use as an electrode in dual-ion ion or anion-ion organic batteries. In addition, the possibility of recovering the molecular material by dissolving it directly in an organic solvent from cycled electrodes was demonstrated. Thanks to this approach, the recycled active material could be reused directly in new cells, which showed decent performance, but with room for improvement in terms of the process. These promising results give a strong incentive to continue such studies into the recycling of electrode materials, making it possible to do away with new synthesizing by involving process engineering, for example.

Acknowledgements

The region Hauts-de-France is gratefully acknowledged for financial support through the “Renforcement du stockage de l’énergie” project and grant accorded to M.R. This work was supported by a French government grant from the Agence Nationale de la Recherche under the France 2030 program, reference ANR-23-PEBA-0007. It is available in full text on HAL. Science (CCBY License, Creative Commons). The authors acknowledge the support provided by the HPC resources and allocations of computing time from GENCI (IDRIS) and the facilities of the “Mésocentre de Calcul Informatique Aquitain” (MCIA) of the University of Bordeaux, Pau, and “Pays de l’Adour”.

Conflicts of Interest

The authors declare no conflicts of interest.

Data Availability Statement

The data that support the findings of this study are available from the corresponding author upon reasonable request.

Keywords: anion insertion · energy storage · molecular material · organic electrode material · p-type materials · phenothiazine · recycling

- [1] J. Bordoff, M. L. O’Sullivan, <https://www.foreignaffairs.com/world/energy-insecurity-climate-change-geopolitics-resources>, accessed 2025-04-10.
- [2] P. Poizot, J. Gaubicher, S. Renault, L. Dubois, Y. Liang, Y. Yao, *Chem. Rev.* **2020**, *120*, 6490.
- [3] A. E. Lakraychi, F. Dolhem, A. Vlad, M. Becuwe, *Adv. Energy Mater.* **2021**, *11*, 2101562.
- [4] Y. Ding, C. Zhang, L. Zhang, Y. Zhou, G. Yu, *Chem. Soc. Rev.* **2018**, *47*, 69.
- [5] T. B. Schon, B. T. McAllister, P.-F. Li, D. S. Seferos, *Chem. Soc. Rev.* **2016**, *45*, 6345.
- [6] G. Dai, Y. He, Z. Niu, P. He, C. Zhang, Y. Zhao, X. Zhang, H. Zhou, *Angew. Chem.* **2019**, *131*, 10007.
- [7] C. Wang, X. Li, B. Yu, Y. Wang, Z. Yang, H. Wang, H. Lin, J. Ma, G. Li, Z. Jin, *ACS Energy Lett.* **2020**, *5*, 411.
- [8] K. Lee, I. E. Serdiuk, G. Kwon, D. J. Min, K. Kang, S. Y. Park, J. E. Kwon, *Energy Environ. Sci.* **2020**, *13*, 4142.
- [9] R. Russo, R. Murugesan, A. Jamali, J.-N. Chotard, G. Toussaint, C. Frayret, P. Stevens, M. Becuwe, *ChemNanoMat* **2022**, *8*, e202200248.
- [10] M. Yao, H. Senoh, T. Sakai, T. Kiyobayashi, *J. Power Sources* **2012**, *202*, 364.
- [11] R. Russo, J.-N. Chotard, G. Gachot, C. Frayret, G. Toussaint, P. Stevens, M. Becuwe, *ACS Energy Lett.* **2023**, *8*, 4597.
- [12] A. Wild, M. Strumpf, B. Häupler, M. D. Hager, U. S. Schubert, *Adv. Energy Mater.* **2017**, *7*, 1601415.
- [13] S. I. Etkind, J. Lopez, Y. G. Zhu, J.-H. Fang, W. J. Ong, Y. Shao-Horn, T. M. Swager, *ACS Sustainable Chem. Eng.* **2022**, *10*, 11739.
- [14] A. A. Golriz, T. Suga, H. Nishide, R. Berger, J. S. Gutmann, *RSC Adv.* **2015**, *5*, 22947.
- [15] M. Kolek, F. Otteny, P. Schmidt, C. Mück-Lichtenfeld, C. Einholz, J. Becking, E. Schleicher, M. Winter, P. Bieker, B. Esser, *Energy Environ. Sci.* **2017**, *10*, 2334.
- [16] B. M. Peterson, C. N. Gannett, L. Melecio-Zambrano, B. P. Fors, H. Abruna, *ACS Appl. Mater. Interfaces* **2021**, *13*, 7135.
- [17] V. Perner, D. Diddens, F. Otteny, V. Kupers, P. M. Bieker, B. Esser, M. Winter, M. Kolek, *ACS Appl. Mater. Interfaces* **2021**, *13*, 12442.
- [18] M. Armand, P. Axmann, D. Bresser, M. Copley, K. Edström, C. Ekberg, D. Guyomard, B. Lestriez, P. Novák, M. Petraníková, W. Porcher, S. Trabesinger, M. Wohlfahrt-Mehrens, H. L.-I. B. Zhang, *J. Power Sources* **2020**, *479*, 228708.
- [19] R. Murugesan, B. Matthieu, F. Dolhem, *ChemSusChem* **2020**, *13*, 2364.
- [20] R. Chen, D. Bresser, M. Saraf, P. Gerlach, A. Balducci, S. Kunz, D. Schröder, S. Passerini, J. Chen, *ChemSusChem* **2020**, *13*, 2205.
- [21] É. Deunf, P. Moreau, É. Quarez, D. Guyomard, F. Dolhem, P. Poizot, *J. Mater. Chem. A.* **2016**, *4*, 6131.

Manuscript received: July 18, 2025
Version of record online: